

MFC/IMC SCHEME AS A FAULT TOLERANT CONTROL STRUCTURE

Jerzy BRZÓZKA

Maritime University of Szczecin, Department of Vessel's Control Systems
 70-205 Szczecin, Podgórna 51/53 St., Poland; jb@am.szczecin.pl

Summary

The paper deals with the fault tolerant control in two-loop control system structure (MFC/IMC, *Model Following Control/Internal Model Control*). System consists of the model of a nonlinear plant (main ship engine) and two PID controllers. In distinction from other works on this subject (the MFC/IMC structure), special attention was paid to robustness of the linearized structure to perturbations caused by the plant parameters changes, different uncertainties, changes of the operating points and tuning parameters of the controllers as well as catastrophic failures formed in the considered structure. The simulations carried out in MATLAB®/Simulink® software.

Keywords: robust control, fault tolerant control, process perturbation, model following control (MFC).

ODPORNY NA USZKODZENIA UKŁAD REGULACJI TYPU MFC/IMC

Streszczenie

Artykuł dotyczy regulacji odpornej w dwu pętlowej strukturze MFC/IMC zawierającej model nieliniowego obiektu regulacji (prędkości obrotowej wału okrętowego silnika głównego) i dwa regulatory PID. W odróżnieniu od innych prac na temat struktury MFC/IMC, w artykule tym szczególną uwagę zwrócono na odporność struktury zlinearyzowanej na perturbacje parametrów regulowanego procesu, odporność na perturbacje spowodowane różnymi zaburzeniami, np. wywołanymi zmianami punktów pracy obiektu, parametrami regulatorów lub uszkodzeniami katastroficznymi struktury. Symulacje zostały wykonane w programie MATLAB®/Simulink®.

Słowa kluczowe: regulacja odporna, regulacja tolerująca uszkodzenia, perturbacje procesu, regulacja śledząca z modelem.

1. INTRODUCTION

Fault tolerance of dynamic systems can be achieved either from system robustness to faults and other uncertainties, or from controller reconfiguration or restructuring in response to special faults. Actually, a well-designed control system may have some fault tolerance capabilities what can be designed (e.g., by properly choosing feedback gains) to compensate for some system uncertainties such as disturbances and noise, and the fault can be considered as a kind of system uncertainty. This paper proposes a fault-tolerant control strategy for fault based on the use of MFC/IMC structure. There is no need to design special diagnostic observers which is the main advantage of this structure.

2. PROPERTIES OF A LINEAR MFC/IMC STRUCTURE

According to [5] the MFC/IMC structure is shown in Fig. 1.

The special advantage of MFC/IMC structure is that the model $M(s)$ does not have to be exactly equal to the process $P(s)$, because in such a situation the process $P(s)$ is controlled by the sum of two components: control signals from $R_m(s)$ and

$R(s)$ controllers. If $M(s) = P(s)$ then $R(s)$ controller does not work and presented structure acts as a classical fixed value control loop. This structure is often described as the system with two-degree-of-freedom (2DOF).

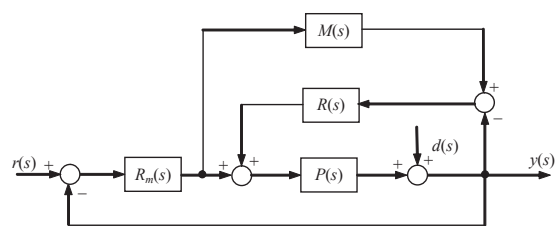


Fig. 1. General block diagram of MFC/IMC structure, where individual transfer functions mean: $M(s)$ – model, $P(s)$ – plant, $R_m(s)$ – model controller, $R(s)$ – plant controller and $r(s)$ – set point value, $y(s)$ – process controlled value, $d(s)$ – disturbances

Plant transfer function $P(s)$ is given by Eq. (1):

$$P(s) = M(s)(1 + \Delta(s)), \quad (1)$$

where $\Delta(s)$ is plant perturbations.

Functions S and T have been assumed as measures of robustness and IAE (*Integral of the Absolute Error*) criterion for step responses as a performance index. The simulations and calculations were carried out in MATLAB.

On the basis of Fig. 1, the process controlled value $y(s)$ is given by Eq. (2):

$$y(s) = r(s)S(s) + d(s)T(s), \quad (2)$$

where:

$$S(s) = \frac{R_m(s)P(s)(1 + R(s)M(s))}{1 + P(s)(R_m(s) + R(s) + R_m(s)R(s)M(s))}, \quad (3)$$

is the sensitivity transfer function and

$$T(s) = \frac{1}{1 + P(s)(R_m(s) + R(s) + R_m(s)R(s)M(s))}, \quad (4)$$

is the complementary sensitivity transfer function.

Adding Eq. (3) and Eq. (4) yields equation (5), which represents the relation between sensitivity functions $S(s)$ and $T(s)$:

$$S(s) = 1 - (1 + R(s)P(s))T(s). \quad (5)$$

3. EXEMPLARY MFC/IMC STRUCTURE

As an example, the dynamics of the revolution speed control of the main ship engine (Fig. 2 and Fig. 3) has been considered as a plant.

3.1. Plant

A linearized "real plant" has been created as an approximation of the nonlinear continuous functions f_n (for dead zone) and f_s (for saturation) at the given operating point (A ; op). Linearization of these gives (6):

$$\frac{num}{s^4 + 60.05s^3 + 1203s^2 + 8060s + 400} \quad (6)$$

where values of num of the transfer functions (6) are given in the Table 1.

Table 1. Values of the transfer function numerator (6) at a given operating point A

$A =$	0.05	0.15	0.2	0.5	0.7	0.9	1.2
$num =$	818	1334	1549	2208	2093	1724	1114

Block diagram of the plant is shown in Fig. 2.

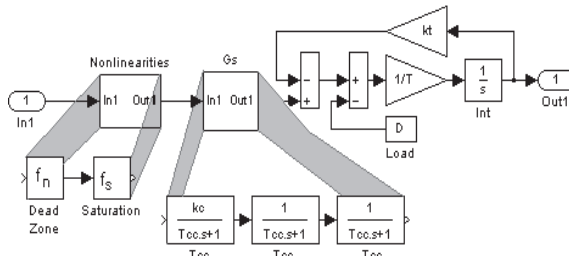


Fig. 2. Block diagram of the nonlinear, continuous "real plant" of the main ship engine (values of plant parameters: $k_c = 0.8$; $T_{cc} = 0.05$ sec; $T = 3$ sec; $k_t = 0.15$)

3.2. Model

The block diagram of a nonlinear model of the main ship engine dynamics is shown in Fig.3 [3]. The same (independently of an operating point) model in the form of the first-order plus time-delay was taken for the process. The time-delay was replaced by second-order Pade approximation. Linearization of the model (Fig. 3) was performed by means of the describing functions $J_n(A)$ for dead zone and $J_s(A)$ for saturation at given operating points.

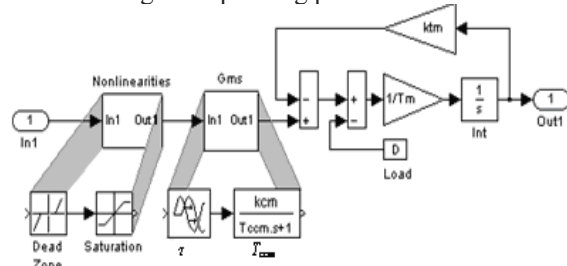


Fig. 3. Block diagram of the nonlinear, non-continuous model for the main ship engine dynamics (values of model parameters: dead zone -0.1 ; 0.1 ; saturation -1.1 ; 1.1 ; $\tau = 0.05$ sec; $k_{cm} = 0.8$; $T_{ccm} = 0.1$ sec; $T_m = 2.5$ sec; $k_{tm} = 0.12$)

3.3. Controllers

Plant controller $R_m(s)$ and correcting controller $R(s)$ have been tuned in *Simulink Response Optimization* toolbox for fully nonlinear MFC/IMC structure. The tuning parameters of the process and correcting PID controllers are: $k_m = 3$; $T_{cm} = 10$ sec; $T_{dm} = 0.7$ sec and $k_k = 1$; $T_{ck} = 5$ sec; $T_{dk} = 0.05$ sec, respectively.

4. ANALYSIS OF EXEMPLARY FAULTS IN MFC/IMC STRUCTURE

4.1. Stability analysis

The stability study of the nonlinear MFC/IMC structures (at different parameters of the process, model or controllers, disconnected outputs of $R(s)$ or $R_m(s)$ controllers, disconnected model's output) has been done by means of the roots computation of the characteristic equations for the given linearized scheme. In these cases, the characteristic equations have the following forms (7 ÷ 10):

for the fully working structure:

$$1 + P(s)(R_m(s) + R(s) + R_m(s)R(s)M(s)) = 0, \quad (7)$$

for disconnected output of R_M :

$$1 + P(s)R(s)(1 + R_m(s)M(s)) = 0, \quad (8)$$

for disconnected output of R (R_m works, only):

$$1 + P(s)R_m(s) = 0, \quad (9)$$

For disconnected output of M :

$$1 + P(s)(R(s) + R_m(s)) = 0. \quad (10)$$

It is easy to notice that characteristic equations (7÷10) are created by rejection of needless components in equation (7). These equations are sometimes called an *interval polynomials*.

All equations fulfill the stability conditions for given parameters.

4.2. ROBUSTNESS ANALYSIS

Robustness analysis of MFC/IMC system has been done for the following exemplary cases:

- Different plant operating points;
- Inaccuracy of the model;
- Inaccurate tuning parameters of controllers;
- Reaction to catastrophic failures, this is disconnection of output $R_m(s)$ and $R(s)$ controllers and model $M(s)$;
- Process parameters perturbations;
- The simultaneous changes of the model and process parameters;
- Linear model use for nonlinear process is presented in [2].

Ad. a) Different plant operating points.

The values of performance index IAE (for signal error in R_m, P control loop) for the different operating points A of the process, and for different approximations of the model and process but for the same tuning parameters of $R_m(s)$ and $R(s)$ controllers are presented in Table 2.

Table 2. Values of IAE for different MFC/IMC structures at given operating points

A^1 (or op)	0.15	0.2	0.5	0.7	0.9	1.2	average value of IAE	relative error for IAE
MFC/IMC	Values of IAE							
non-linear ²	3.58	3.28	3.02	4.10	5.13	7.91	4.50	0%
linear ³	4.73	4.76	4.96	5.10	5.23	5.60	5.06	12.44%
nPIM ⁴	4.35	4.32	4.35	4.44	4.59	6.94	4.83	7.33%

From Table 2 appears that controllers tuned at one operating point work properly at other operating points.

Data presented in Table 2 permit to infer that for designing purposes partially or fully linearized structure can be used instead of nonlinear.

Unit step changes (reference and disturbance signals) for two exemplary operating points are shown in Fig. 4 and Fig. 5. Plant controller $R_m(s)$ and correcting controller $R(s)$ have been tuned in Simulink Response Optimization program for fully nonlinear structure.

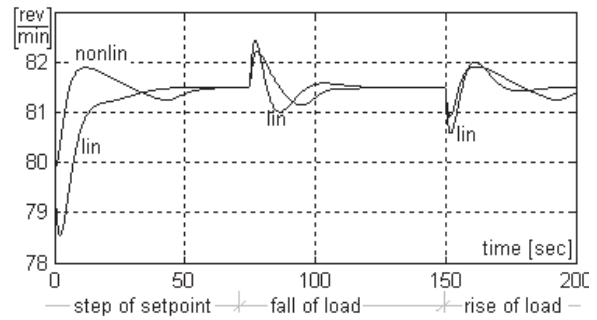


Fig. 4. Step responses for the fully nonlinear and fully linearized structure on unit step changes in the reference and disturbance signals ($A = 0.15$)

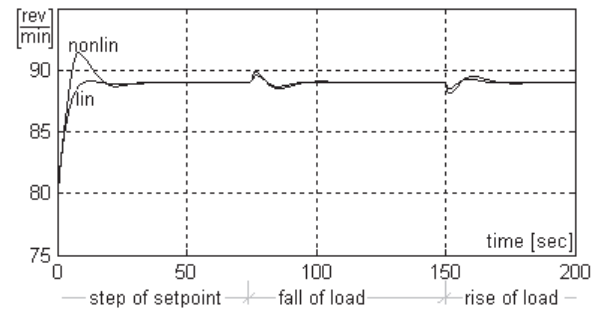


Fig. 5. Step responses for the fully nonlinear and fully linearized structure on unit step changes in the reference and disturbance signals ($A = 0.9$)

Ad b) Inaccuracy of the model.

The analysis of the model inaccuracy has been done by comparison of a maximal and current plant perturbations for model linearized at a given operating point.

In the case of the linearized MFC/IMC structure the maximal admissible perturbations Δ at a given operating point can be expressed in the form of (11) according to [2]:

$$\Delta_{MFC/IMC} < \left| \frac{(1 + R(s)M(s, op))(1 + R_m(s)M(s, op))}{R_m(s)M(s, op)} \right| \quad (11)$$

These admissible perturbations (11) depend on the operating point op due to the nonlinearities in the controlled plant.

Current perturbations $\Delta_{current}$ at a given operating point are given by the following equation (12) according to [2]:

$$\Delta_{current} = \left| \frac{P(s, op)}{M(s, op)} - 1 \right| \quad (12)$$

Therefore, the maximal values of the parameters changes can be determined on the basis of the expressions (11) and (12).

A comparison of the exemplary maximal admissible and current perturbations is shown in Figs. 6, 7.

¹ operating point

² nonlinear plant and model

³ linear plant and model

⁴ nonlinear plant, linear model, nP/M

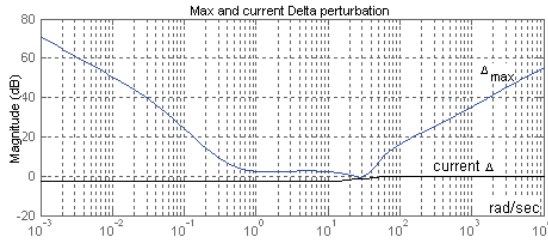


Fig. 6. Maximal and current perturbations Δ for second order Padé approximation of model time-delay; $A = 0.9$; gain coefficient of plant enlarged three times

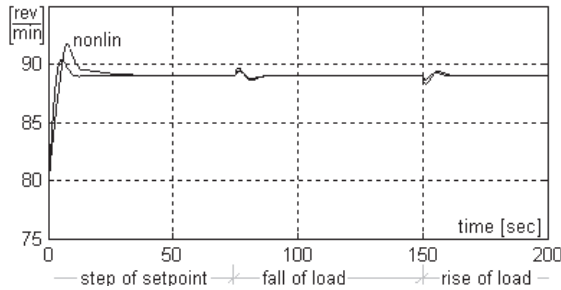


Fig. 7. Step responses of nonlinear and linearized MFC/IMC system on unit step changes in the reference and disturbance signals ($n = 2$; $A = 0.9$; gain coefficient of plant enlarged three times)

As follows from Fig. 6 that the triple increase of the object gain coefficient did not cause the exceeding of the admissible perturbation from the stability point of view, which is also confirmed by the graph in Fig. 7.

Ad. c) Inaccurate tuning parameters of controllers.

For modeling this situation it has been assumed, that the parameters of controllers $R_m(s)$ and $R(s)$ have been replaced accidentally without any changes of other parameters of this structure. The Bode plots (with the gain curves; $A = 0.9$) of maximal and current perturbations in both cases are shown in Fig. 8 and Fig. 9 and step responses for these cases in Fig. 5 and Fig. 10. It follows from the Figs. 8, 9 that the stability conditions are fulfilled.

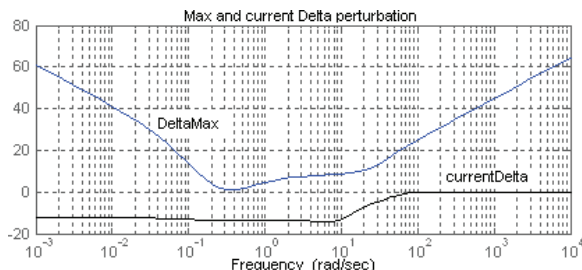


Fig. 8. Bode plot of the maximal and current perturbations (controllers tuned correctly)

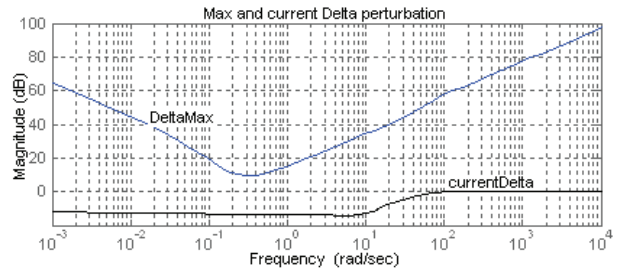


Fig. 9. Bode plot of the maximal and current perturbations for controllers tuned incorrectly

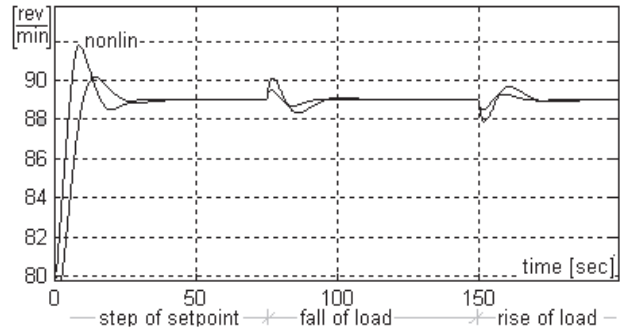


Fig. 10. Unit step responses in MFC/IMC structure with controllers tuned incorrectly ($A = 0.9$; IAE = 5.36 for nonlinear model; IAE = 8.59 for linear model)

Ad. d) Reaction to catastrophic failures.

The failures degenerating MFC/IMC structure (disconnection of output $R_m(s)$ and $R(s)$ controllers and model $M(s)$) has been treated as catastrophic failures.

Block diagram of a control system with disconnected output of $R_m(s)$ controller is shown in Fig. 11, plot of complementary sensitivity function T in Fig. 12 and step responses in Fig. 13.

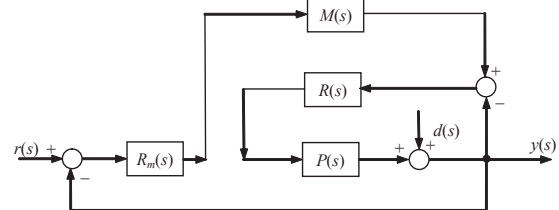


Fig. 11. Disconnection of output $R_m(s)$ controller

In this case, the system in Fig. 11 has the following transfer functions (13) and (14):

Transfer function G_{yr} from set point r to process output y :

$$G_{yr}(s) = \frac{P(s)R_m(s)M(s)R(s)}{1 + P(s)R(s)(1 + R_m(s)M(s))}, \quad (13)$$

Transfer function G_{yd} from load disturbance d to process output y :

$$G_{yd}(s) = \frac{1}{1 + P(s)R(s)(1 + R_m(s)M(s))}, \quad (14)$$

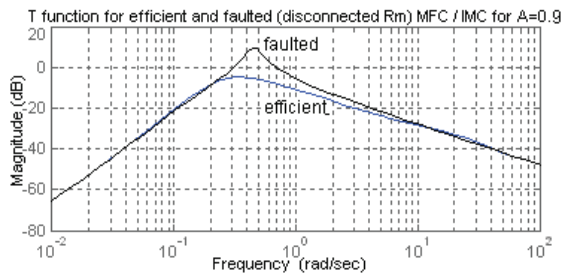


Fig. 12. T function plot for MFC/IMC with disconnected output of R_m and correctly tuned R controller ($A = 0.9$)

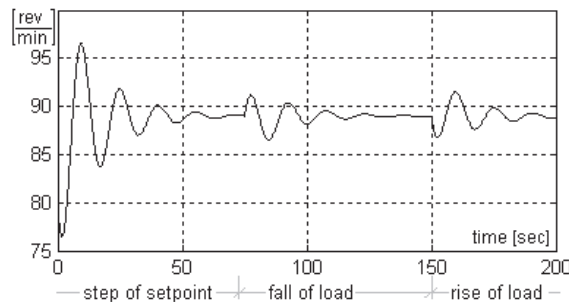


Fig. 13. Unit step response in linear MFC/IMC structure with disconnected output of R_m and correctly tuned R controller ($A = 0.9$; nonlinear structure is unstable)

For disconnected output of the correcting controller $R(s)$, the process is controlled by $R_m(s)$ controller only – the MFC/IMC structure is transformed to fixed-value control loop. Plot of complementary sensitivity functions T is shown in Fig. 14 and step responses in the damaged linear and nonlinear structures in Fig. 15.

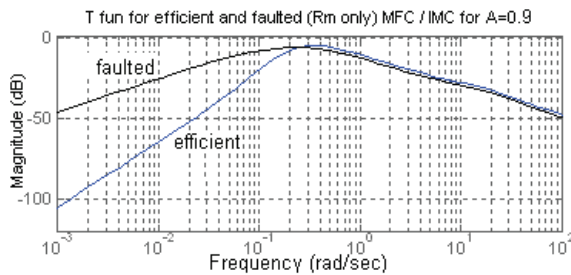


Fig. 14. T function plot for MFC/IMC structure with disconnected output of R and correctly tuned R_m controller ($A = 0.9$)

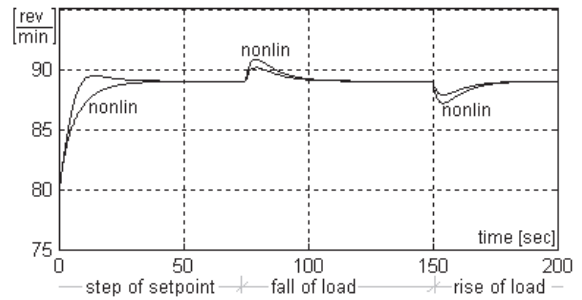


Fig. 15. Unit step responses of linear and nonlinear MFC/IMC structure with disconnected output of R and correctly tuned R_m controller at the operating point $A = 0.9$

Block diagram of a control system with disconnected output of model $M(s)$ is shown in Fig. 16, unit step responses in Fig. 17 and plot of complementary sensitivity functions T in Fig. 18.

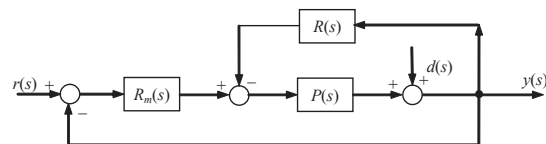


Fig. 16. Block diagram of a control system without model $M(s)$

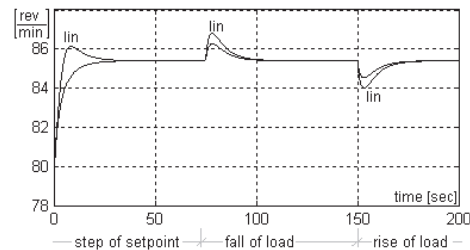


Fig. 17. Unit step responses of linear and nonlinear MFC/IMC structure without model and correctly tuned R and R_m controllers at $A = 0.9$

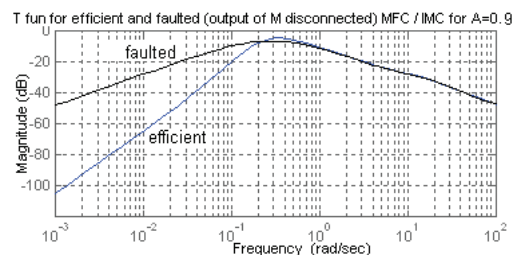


Fig. 18. T function plot for MFC/IMC with disconnected output of M and correctly tuned controllers at the operating point $A = 0.9$

From the graphs in Figs. 12, 14 and 18 it follows that disconnection of the output controller $R_m(s)$ (Fig. 12) slightly changes the properties of the MFC/IMC structure from disturbances rejection point of view. In remaining cases (disconnection of the controller $R(s)$ – Fig. 14; disconnection of the model $M(s)$ – Fig. 18) rejection disturbances are worse in low frequency range.

Ad. e) Process parameters perturbations.

The following exemplary simulation experiments were conducted in this case:

- Five-times enlargement of the process time constant – Fig. 19 and Fig. 20.

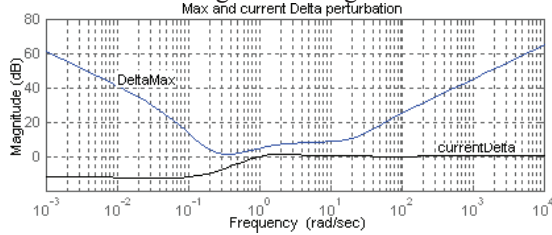


Fig. 19. T function plot for MFC/IMC (five-times enlargement of process time constant, correctly tuned controllers, $A = 0.9$)

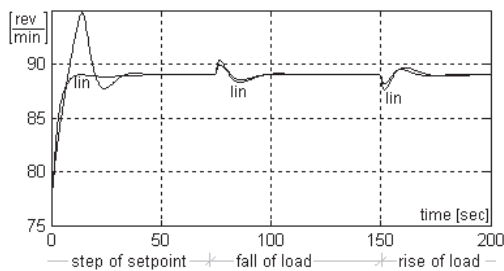


Fig. 20. Unit step responses in linear and nonlinear structure for five-times enlargement of process time constant, correctly tuned controllers and at the operating point $A = 0.9$

- Five-times enlargement of the process time constant and disconnected output of the controller $R(s)$ – Fig. 21 and Fig. 22.

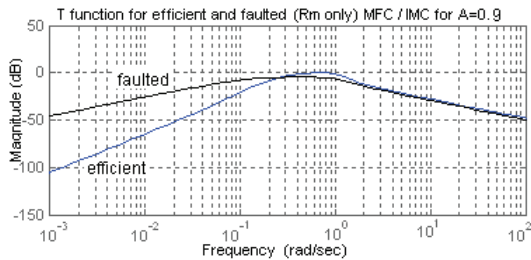


Fig. 21. T function plot for five-times enlargement of process time constant, disconnected R controller and correctly tuned R_m controller, $A = 0.9$)

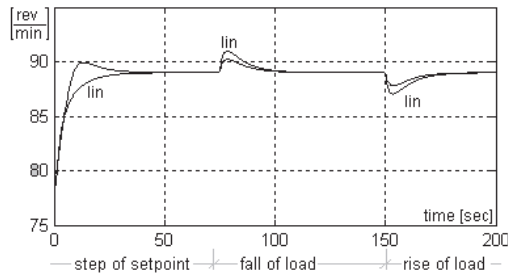


Fig. 22. Step responses for five-times enlargement of process time constant, disconnected R and correctly tuned R_m controller, ($A = 0.9$)

- Five-times enlargement of the process time constant and disconnected output of the model $M(s)$ – Fig. 23 and Fig. 24.

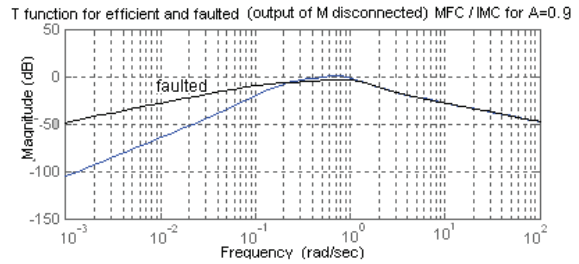


Fig. 23. T function plot for MFC/IMC for five-times enlargement of process time constant, correctly tuned controllers, disconnected model, $A = 0.9$

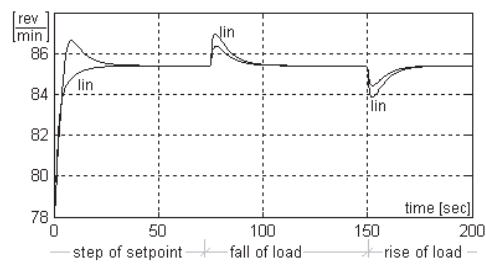


Fig. 24. Step responses of linear and nonlinear structure (five-times enlargement of process time constant, correctly tuned controllers, disconnected model, $A = 0.9$)

Ad. f) The simultaneous change of the model and process parameters.

The triple enlargement of the object gain coefficient k_c as well as simultaneous 3.5 enlargement of the model gain coefficient k_{cm} in the linear and nonlinear MFC/IMC structure (for $A = 0.9$) does not vary the step responses: performance index IAE for nonlinear system is equal to 1.53 and 1.54 for linear.

If the object gain coefficient k_c is enlarged four times, and simultaneously the model gain coefficient k_{cm} will stay without changes ($k_{cm} = 0.8$), the values of the IAE are equal to (for $A = 0.9$): 2.08 for nonlinear system (if $k_c = k_{cm} = 0.8$ IAE is equal to 5.13) and 3.46 for linear system (if $k_c = k_{cm} = 0.8$ IAE is equal to 5.23).

If the object gain coefficient k_c is enlarged twice (for larger gains nonlinear system is unstable) and simultaneously the model gain coefficient k_{cm} will stay without changes ($k_{cm} = 0.8$) then the values of the IAE criterion are equal to (for $A = 0.9$): 5.25 for nonlinear and 4.35 for linear systems.

5. CONCLUSIONS

The carried out research allows to consider MFC/IMC structure as fault tolerant control. It is robust for the following perturbations:

- 1) Changes of operating points in the case of nonlinear process (Figs. 4, 5);

- 2) Model inaccuracy (Figs. 6, 7); model inaccuracy has been simulated by changes of the process gain coefficient;
- 3) Wrong tuning parameters of controllers (Figs. 8, 9);
- 4) Catastrophic failures denote the degenerating structure MFC/IMC (see section 4.2.d and Figs. 23, 24) with exception of the situation with disconnected model $M(s)$, because MFC/IMC transforms into fixed-value control loop.
- 5) Changes of the process parameters (Figs. 19, 20);
- 6) Changes of the process parameters with simultaneous disconnecting of the correcting controller (Figs. 21, 22);
- 7) Simultaneous changes of parameters of the process and model.

REFERENCES

- [1] Brzózka J.: *Układ regulacji prędkości obrotowej typu MFC z regulatorem rozmytym*, Zeszyty Naukowe Wyższej Szkoły Morskiej w Szczecinie nr 71, 2004, pp. 89-99.
- [2] Brzózka J.: *Analysis of nonlinear MFC/IMC structure for a ship engine speed control*, V Konferencja Explo-Ship 2008, submitted for publication.
- [3] Kowalski Zb.: *Badania symulacyjne podsystemów napędowych statku*, Zeszyty Naukowe Politechniki Gdańskiej, Elektryka nr 49, 1980.
- [4] Masanori I. et al.: *Main engine revolution control for ship with direct drive volume control system*, Proceedings of the 6th International Symposium on Marine Engineering Tokyo, 2000.
- [5] Skoczowski S. et al.: *Odporna regulacja PID o dwóch stopniach swobody*, Warszawa, PWN-MIKOM 2006.

Acknowledgments

The author would like to thank Teresa Kurowska, Ph. D. Eng. for her valuable suggestions and comments which help improve this paper.



BRZÓZKA Jerzy received his Ph.D.Eng. degree in automatic control in 1982. He is currently Head of Department of Vessel's Control Systems in the Maritime University of Szczecin (Poland). His current research interests include robust, PID, intelligent and fault-tolerant control.